Comparison of Strength and Young Modulus of Aligned Discontinuous Fibre PLA Composites Obtained Experimentally and from Theoretical Prediction Models

M.G Aruan Efendy[a] and K. L. Pickering[b]

[a] Faculty of Civil Engineering, Universiti Teknologi MARA, Malaysia

[b] Faculty of Science and Engineering, University of Waikato, New Zealand

Corresponding author:

M.G. Aruan Efendy

E mail address: mghazali_ae@yahoo.com

ABSTRACT

The present paper describes work carried out to compare the strength performance of PLA reinforced aligned discontinuous harakeke and hemp fibre mat composites evaluated experimentally and using various simple elastic mathematical prediction models. Fibre mats were produced by means of Dynamic Sheet Former (DSF), and stacked alternately with PLA sheets to produce composites with up to 40 wt% fibre content. The fibre content was increased from 5 wt% to 40 wt% using 5 wt% interval. In this work, both harakeke and hemp composites were manufactured using hot-press. It was found that, better agreement to the experiment was obtained for Young's modulus compared to those composite strengths. The Modified Rule of Mixtures is found to give accuracy within 41% for strength, while the Cox model showing the best agreement (<10%) for Young's modulus for fibre contents up to 25wt%. Better agreement obtained for Young's modulus is believed to due to less mechanism involved at where Young's modulus is measured.

KEYWORDS:

Discontinuous Reinforcement; Dynamic Sheet Former; Aligned Fibre; Composite Modelling; Thermoplastic Composites

1. INTRODUCTION

Natural-fibre-reinforced bio-derived polymer matrix composites, commonly referred to as bio-composites, have gained renewed interest over the past few decades because of their low material costs, low densities, high specific moduli and environmentally friendly appeal, as well as their low production energy requirements [1]. The natural fibres used are renewable, non-abrasive, can be incinerated for energy recovery and they give less concern regarding health and safety during handling than synthetic fibres. Their excellent price-performance ratios at low weight in combination with their low environmental impact has resulted in increasing uptake by engineering markets such as the automotive and construction industries. Studies have been carried out internationally to assess the possibility of using natural fibre-composites for non-structural and structural applications. Assessment of tensile properties of manufactured composites are often carried-out using various mechanical tests. Although some simple mathematical prediction models are found to be used and give good approximations, but they are often used to predict tensile properties of continuous fibre composites. Tensile properties of composites reinforced with continuous and uniaxially aligned fibres can be predicted reasonably accurate using simple Rule of Mixtures equations. Generally, in the prediction, both fibre and matrix are assumed to be elastic and strain in the fibre and the matrix is also assumed to be the same. However, when the fibres are discontinuous, equations given by the Rule of Mixtures are not anymore obeyed. In discontinuous fibre composites, tensile properties are largely affected by a number of parameters such as fibre length, fibre orientation, fibre dispersion and stress transfer between fibre and matrix. Of these, the fibre orientation and stress

transfer are strongly related to the optimum tensile properties of the composite. A number of models have been developed to predict the composite tensile properties taking into consideration aforementioned factors, however, large spectrum of disparity is observed. In this paper, tensile properties of PLA composites reinforced with dynamically sheet formed harakeke and hemp fibre mats using hot press were compared with the predicted values using various models and the parameters of mechanism controlling strength were comprehensively discussed and compared.

2. THEORETICAL MODELLING OF COMPOSITE TENSILE PROPERTIES

Micromechanical models have been shown to be a useful method for predicting strength and Young's modulus of continuous and discontinuous fibre composites [2]. Commonly, the basic Rule of Mixtures is used to predict strength and Young's modulus of composites reinforced with unidirectional continuous fibre in parallel and perpendicular to the loading direction. However, strength and Young's modulus prediction is more complex for discontinuous fibre composites that commonly have fibre with varying length and orientation. In this paper, the main prediction models are presented, starting with the basic Rule of Mixtures followed by models developed to predict tensile properties of discontinuous fibre composites.

2.1 Rule of Mixtures Models (Parallel and Series)

The Parallel and Series Rule of Mixtures models [3] are the most commonly applied models to represent the upper and lower bounds for strength and Young's modulus of unidirectional continuous fibre composites. It is assumed that reinforcing fibres have perfect interfacial bonding with the matrix and iso-strain conditions exist for fibre and matrix. According to these models, strength and Young's modulus are calculated using the following equations:

Parallel model (parallel to fibre direction):

$$\sigma_c = \sigma_f V_f + \sigma_m V_m \quad (1)$$

$$E_c = E_f V_f + E_m V_m \quad (2)$$

Series model (90° to fibre direction):

$$\sigma_c = \frac{\sigma_m \sigma_f}{\sigma_m V_f + \sigma_f V_m} \quad (3)$$

$$E_c = \frac{E_m E_f}{E_m V_f + E_f V_m} \quad (4)$$

where σ, E and V are strength, Young's modulus and volume fraction respectively. The subscripts c, m and f represent composite, matrix and fibre, respectively. Since the composites in this work were designed according to weight fractions and the above equations rely on fibre volume fraction, in order to be able to use them, the fibre and matrix volume fractions (V_f and V_m) needed to be calculated from the fibre weight fraction (W_f) using the following equations:

$$V_f = \frac{1}{1 + \frac{\rho_f (1 - W_f)}{\rho_m \quad W_f}} \quad (5)$$

$$V_m = 1 - V_f \quad (6)$$

such that ρ_f and ρ_m are density of fibre and matrix respectively [4]. It should be realised that there is the possibility that the actual matrix density may vary due to the presence of the fibres for a number of reasons (e.g. nucleation of matrix crystallinity at fibre surfaces or effects due to dissolution and reaction with sizing where this is present) which therefore results in a slight variation in calculated fibre volume fraction compared to the actual fibre volume fraction [5].

2.2 Hirsch's Model

Hirsch's model [6] is based on a combination of the Parallel and Series models and can be applied to discontinuous and variably oriented fibre composites. It is fitted empirically to experimental data by means of a fitting parameter, *x* (between zero to one) as seen in Equations 7 and 8, which can be considered to represent the stress transfer efficiency between fibre and matrix taking into account the fibre orientation, fibre length and stress amplification at fibre ends.

$$\sigma_c = x\ \sigma_m V_m + \sigma_f V_f\ + (1-x)\frac{\sigma_f \sigma_m}{\sigma_m V_f + \sigma_f V_m} \tag{7}$$

$$E_c = x\ E_m V_m + E_f V_f\ + (1-x)\frac{E_f E_m}{E_m V_f + E_f V_m} \tag{8}$$

This model has been found to give a good fit with actual composite strengths and Young's moduli [7].

2.3 Halpin-Tsai Model

The Halpin and Tsai model [8, 9] is a semi-empirical model that can be applied to tensile strength and Young's modulus of discontinuous fibre reinforced composites aligned in either the longitudinal or transverse direction as follows:

$$\sigma_c = \sigma_m \frac{1 + \zeta \eta V_f}{1 - \eta V_f} \tag{9}$$

$$E_c = E_m \frac{1 + \zeta \eta^* V_f}{1 - \eta^* V_f} \tag{10}$$

where η and η^* are given by:

$$\eta = \frac{\frac{\sigma_f}{\sigma_m} - 1}{\frac{\sigma_f}{\sigma_m} + \zeta} \tag{11}$$

$$\eta^* = \frac{\frac{E_f}{E_m} - 1}{\frac{E_f}{E_m} + \zeta} \tag{12}$$

and ζ is a shape fitting parameter to fit the Halpin–Tsai model to experimental data depending on fibre geometry and loading direction (longitudinal or transverse to fibre direction). ζ for circular-sectioned fibre is commonly given by:

$$\zeta = \frac{2l}{d} \tag{13}$$

where l is the length of the fibre in the direction of the load, d is the diameter of the fibre (such that ζ can be taken as 2 for transverse tensile properties) [2, 10-12]. The Halpin-Tsai model was further modified by Nielsen [13] taking into consideration a factor to account fibre arrangement as well as fibre content, ψ to enable a better prediction as given by the following equations:

$$\sigma_c = \sigma_m \frac{1 + \zeta\eta V_f}{1 - \eta\psi V_f} \tag{14}$$

$$E_c = E_m \frac{1 + \zeta\eta^* V_f}{1 - \eta^*\psi V_f} \tag{15}$$

and

$$\psi = 1 + \frac{1 - \phi_{max}}{\phi_{max}^2} V_f \tag{16}$$

where $ø_{max}$ is the maximum fibre packing fraction for the relevant fibre arrangement and has a value 0.785 for a square arrangement of fibres, 0.907 for a hexagonal array of fibres and 0.82 for random packing of fibres [6].

2.4 Cox Model

Cox's model [14] is amongst the earliest models used to predict the strength and Young's modulus of composites reinforced with aligned discontinuous fibres. It assumes that the interface between fibres and matrix is perfect, with both fibre and matrix perfectly elastic and isotropic. This model is developed based on shear-lag theory which considers stress transfer into discontinuous fibre occurring by shear stress at the fibre/matrix interface when the fibre of length, *l* embedded in a matrix subjected to a strain in fibre direction. Shear stress is a maximum at the fibre ends and, decreases to zero at the centre which leads to a tensile stress profile within the fibre of zero at the fibre ends, increasing towards the middle of the fibre, limited by the breaking stress of the fibre [3, 10, 15, 16]. If the fibre is long enough, as the strain in the composite increases, eventually, the maximum stress at the centre of the fibre will reach the tensile strength of the fibre and fibre failure will occur. However, for shorter fibre, fibre failure does not occur. In this instance, debonding would be expected, which will lead to pull-out during composite failure. According to this model, strength and Young's modulus of a composite can be predicted similarly to the Rule of mixtures by including a factor to account for the effectiveness of load transfer from matrix to fibre giving:

$$\sigma_c = \sigma_f V_f \left(1 - \frac{\tanh\left(\frac{\beta l}{2}\right)}{\frac{\beta l}{2}}\right) + \sigma_m V_m \tag{17}$$

$$E_c = E_f V_f \left(1 - \frac{\tanh\left(\frac{\beta l}{2}\right)}{\frac{\beta l}{2}}\right) + E_m V_m \tag{18}$$

where

$$\beta = \left(\frac{2\pi G_m}{E_f A_f l \ln\frac{R}{r}}\right)^{\frac{1}{2}} \tag{19}$$

where r is radius of the fibre, G_m is the shear modulus of matrix, l is length of fibre and A_f is the area of the fibre and R is centre to centre distance of the fibres [17].

For hexagonally packed fibres,

$$R = \left(\frac{2\pi r^2}{\sqrt{3}V_f}\right)^{\frac{1}{2}} \tag{20}$$

and for square packed fibres,

$$R = r\left(\frac{\pi}{4V_f}\right)^{\frac{1}{2}} \tag{21}$$

If ($\beta l/2$) is large, the value of reinforcement effectiveness reduction factor approaches unity, but if ($\beta l/2$) *is* small, it tends to zero [18]. Cox's model was further extended by Krenchel [19] to take into account fibre orientation by adding a fibre orientation factor, K_θ into the basic Cox model giving:

$$\sigma_c = \sigma_f V_f K_\emptyset \left(1 - \frac{\tanh\left(\frac{\beta l}{2}\right)}{\frac{\beta l}{2}}\right) + \sigma_m V_m \tag{22}$$

$$E_c = E_f V_f K_{\emptyset}\left(1 - \frac{\tanh\frac{\beta l}{2}}{\frac{\beta l}{2}}\right) + E_m V_m \quad (23)$$

$K_{\emptyset}$ has a value of unity for axially aligned fibre composites, 0.375 for planar random configuration and 0.2 for a three dimensional randomly oriented fibre composites [15, 20, 21].

2.5 Kelly - Tyson Model

The Rule of Mixtures model for fibres parallel to loading direction was modified using a different approach by Kelly and Tyson to predict the strength and Young's modulus of axially aligned discontinuous fibre composites [3]. It is derived based on stress distribution along the fibre embedded in an elastic-plastic matrix. The applied load is assumed to be transferred to the fibres by means of shear forces at the fibre-matrix interface as described for the Cox model, but the stress increases linearly with distance from the fibre ends up to yield stress, at which the shear stress at the interface is assumed to be constant until the strain in the fibre is equal to that in the matrix of which the fibre stress levels out and the shear stress at the interface is zero (Figure 1) [14]. In this model, an average fibre length relative to a fibre length termed the critical fibre length is considered. The critical fibre length (L_c) is defined as the minimum length at which the stress in the fibre can reach the tensile strength (σ_f). It can be determined experimentally and/or can be determined using micromechanics such as through a model proposed by Bowyer-Bader [22, 23]. The most common techniques used are the fibre fragmentation test [24] or a pull-out test [25] such that the critical fibre length can be determined using the following equation:

$$L_c = \frac{\sigma_f D}{2\tau} \quad (24)$$

where, D is the mean fibre diameter and τ is the interfacial shear strength. It is obvious that the improvement of interfacial shear strength results in lower critical fibre lengths. For a fibre having length equal to L_c, the ultimate fibre tensile stress is only achieved at the centre of the fibre (see Figure 1). As fibre length increases to $L > L_c$, the fibre reinforcement becomes more effective and the ultimate tensile stress could be achieved within the fibre over a greater length. Fibre lengths less than the critical fibre length L_c, cannot be broken and will eventually debond and be pulled out of the matrix.

Figure 1

According to this model, the strength and Young's modulus of a composite depends on a fibre stress transfer factor, denoted as K_{st} which determines the stress transfer efficiency from matrix to fibres; dependent on whether the average fibre length (L) is longer than L_c or shorter than L_c such that:

$$\sigma_c = \sigma_f V_f K_{st} + \sigma_m V_m \tag{25}$$

$$E_c = E_f V_f K_{st} + E_m V_m \tag{26}$$

with K_{st} determined using the following equations:

$$K_{st} = \frac{L}{2L_c} \qquad \text{for } L < L_c \tag{27}$$

or

$$K_{st} = 1 - \frac{L_c}{2L} \qquad \text{for } L > L_c \tag{28}$$

Therefore, the tensile strength and Young's modulus of composites containing fibre shorter than L_c is thus given by:

$$\sigma_c = \sigma_f V_f \frac{L}{2L_c} + \sigma_m V_m \quad (29)$$

$$E_c = \sigma_f V_f \frac{L}{2L_c} + E_m V_m \quad (30)$$

and the tensile strength and Young's modulus of composite containing fibre longer than L_c is given by:

$$\sigma_c = \sigma_f V_f \left(1 - \frac{L_c}{2L}\right) + \sigma_m V_m \quad (31)$$

$$E_c = \sigma_f V_f \left(1 - \frac{L_c}{2L}\right) + E_m V_m \quad (32)$$

The Kelly-Tyson model has been further modified to account a different the fibre orientation [5, 26, 27]. The fibre orientation factor (K_θ) was fitted to the model giving the following which is commonly called the Modified Rule of Mixtures (MROM) as previously mentioned:

$$\sigma_c = \sigma_f V_f K_{st} K_\Theta + \sigma_m V_m \quad (33)$$

$$E_c = E_f V_f K_{st} K_\Theta + E_m V_m \quad (34)$$

The common values for K_θ for respective fibre direction are as given in Cox model.

3. EXPERIMENTAL

Harakeke fibre treated with 5 wt% sodium hydroxide (NaOH) and 2 wt% sodium sulphite (Na_2SO_3) and hemp fibre treated with 5 wt% sodium hydroxide (NaOH) were used to produce fibre mats [28]. In this work, the average length of harakeke and hemp fibres after treatments is 0.625 and 0.765 mm respectively [29]. The diameter of harakeke and hemp fibres was found to be 11.2 and 29.2 mm. The tensile strength and Young's Modulus of harakeke is 782 MPa and 21.3 GPa while for hemp is 911.3 MPa and 26.4 GPa respectively [30]. Aligned fibre mats were produced using a Canpa ADSF dynamic sheet former (DSF) shown in Figure 2.

Figure 2

Production procedure of the fibre mats has been comprehensively described in previously published work [31]. NatureWorks® 3052D injection moulding grade PLA (polylactide) polymer with a density of 1250 kg/m^3 from Nature Works LLC, USA was used as a thermoplastic matrix. Samples of dried harakeke and hemp fibre mats produced in this work are shown in Figure 3.

Figure 3

They were weighed and arranged in a stack (in between Teflon sheets to prevent sticking to mould) with relative numbers of each based on the required fibre weight percentage. Stacks were heated and pressed in a hot press at 170 ℃ and pressed for 3 minutes at 3 MPa. The produced composites were carefully selected and ones with uniform fibre distribution and no air trapped were chosen for testing. Figure 4 shows typical composite samples for testing before and after cutting. The sample size for all sample were 150 mm x 15 mm x 2 mm (approximately).

Figure 4

Prior to tensile testing, all specimens were placed in a conditioning chamber at 23°C ± 3°C and 50% ± 5% relative humidity for at least 48 hours [31]. Tensile testing followed the procedures detailed in ASTM D 638-03; Standard Test Method for Tensile Properties of Plastics, was carried out using 5 kN load cell. An Instron 2630-112 extensometer was attached to the central part of the test specimen to measure the specimen extension. At least 5 replicate samples were

tested for each batch at a constant rate of 2 mm/min. Only sample that fractured within gauge length were considered and tensile strength and Young's moduli were averaged. Typical failure mode of the samples can be seen in Figure 5.

Figure 5

4. RESULTS AND DISCUSSION

4.1 Composite Tensile Properties

Figure 6 presents typical stress versus strain graphs for composites with 15wt% fibre along with that for neat PLA for comparison purposes. It can clearly be seen that, both harakeke and hemp composites failed in a brittle manner at low strain without noticeable yielding. Note that, in this work it was observed that the maximum failure strains for all samples were less than 2 %.

Figure 6

Tensile strengths for harakeke and hemp composites versus fibre content are presented in Figure 7. Clearly, the inclusion of fibres up to 30 wt% for harakeke and 25 wt% for hemp increased the tensile strength of the composites. Reduction in tensile strength for hemp composites with 5 wt% fibre is thought to be due to the fibre content being lower than that referred to as the critical fibre volume fraction for effective reinforcement [31]. Both harakeke and hemp composites failed in brittle manner at low strain. Maximum tensile strengths of harakeke and hemp composites were 101.6 MPa and 87.3 MPa respectively, which were approximately 90 and 60% higher than for PLA (53.9 MPa) with small standard deviations observed, as indicated by the error bars, suggesting good uniformity of fibre distribution throughout the composite.

Higher improvement in tensile strength for harakeke composites could be due to a larger interfacial area as a result of smaller diameter fibres, overweighing the higher tensile strength of the fibre and the more round of harakeke fibre. Reduction of strength above 30 wt% for harakeke and 25 wt% for hemp could be due to insufficient polymer for adequate wetting and increased possibility of fibre-fibre interaction resulting in fibre agglomeration [32], as well as an increase in the structural porosity component in the composite [33]. Although the porosity of the fibre is unlikely to be controlled due to its nature form, but better wetting and lower degree of fibre-fibre interaction can be achieved using polymers with lower viscosity [34].

Figure 7

Young's moduli of harakeke and hemp composites are shown in Figure 8. It can be seen that Young's modulus improved linearly with increasing fibre content up to 30 and 25 wt% for harakeke and hemp fibre composites respectively. This is expected due to the fact that fibre possesses higher Young's modulus than PLA [35, 36].

Figure 8

Improvement in Young's moduli for harakeke and hemp were approximately 120% (8.02 GPa) and nearly 165% (9.67 GPa) at 30 and 40 wt% respectively, compared to that for PLA (3.6 GPa). It may be seen that at the same fibre contents, Young's moduli for hemp composites are higher than that harakeke composites, reflecting the higher Young's modulus for hemp fibre compared to harakeke [36]. This trend has been also found elsewhere [37, 38], which suggests that Young's modulus is less dependent on fibre orientation and fibre/matrix interface but more on fibre content, a higher fibre content providing increased constraint within the matrix.

4.2 Theoretical Modelling – Comparison between the Predicted and Actual Composites Tensile Properties

Figure 9 shows a comparison between the fitted (the Hirsch and Modified Halpin-Tsai ($\zeta = 2$)), predicted (the Cox, Modified Cox, Halpin-Tsai ($\zeta = 2(l/d)$) and MROM) and the experimental composite strengths for harakeke and hemp composites at different fibre contents. Fitting parameters x = 0.13 for the Hirsch was found to give good correlation with the experimental strengths. This x value is relatively consistent with that found for aligned discontinuous sisal fibre LDPE composites (0.15) [7] and higher as would be expected due to better fibre orientation, than those reported for discontinuous fibre composites produced by injection moulding [39] or hot pressed composites with randomly oriented fibre mats (0.09 – 0.1) [7, 40-43]. Note that, the average fibre orientation factors obtained for harakeke and hemp in this study are 0.44 and 0.33 respectively, supporting better correlation with aligned discontinuous fibre composites than randomly oriented fibre composites [29]. For the Modified Halpin-Tsai model, it can be seen that large disparity between the predicted and the experimental values is obtained when ζ according to Equation 13 is used (111 for harakeke and 52 for hemp). Discrepancy is not surprising given that this factor is used for composites with fibres that are perfectly aligned to the loading direction. Much better agreement to the experimental strengths is obtained using $\zeta = 2$, which matches with that generally found to fit experimental composite strengths for discontinuous random fibre composites [2, 7].

Figure 9

As can be seen in Figure 9, using ζ according to the Equation 13 would predict strengths up to about 2.2 times higher than that predicted using $\zeta = 2$, suggesting that if an orientation factor (K_θ) of approximately 0.45 (1/2.2) were applied, good agreement would be obtained. However,

this value varies by 12% and 19% respectively from those achieved for harakeke and hemp fibre using the Bowyer-Bader model. It should be kept in mind that the Modified Halpin-Tsai is a simple model and does not take into account failure mechanisms and in particular stress concentrations as a result of fibre orientation and fibre ends as well as fibre debonding which would be believed to influence the predicted strengths and the calculated K_θ.

Large disparity (up to 280%) is also seen for the strength predicted using the Cox model, larger than that found for other short aligned natural fibre composites (35%) [7]. However, large disparity is again not surprising given that this model assumes that fibres are perfectly aligned and the interface between fibres and the matrix is perfect. However, harakeke and hemp fibres used in this work are not perfectly aligned, and at high stress where the strength is measured, fibre debonding is most likely to occur and stress transfer is expected to be much lower even than for an imperfectly bonded interface [29].

A weakness regarding the predictions of composite strength conducted in this work using the Modified Cox and MROM models is that K_θ values as well as K_{st} are obtained from the Bowyer-Bader model using experimental values of composite strength. However, it is possible to avoid this; K_θ can also be obtained without mechanically testing composites through imaging to find fibre angle using the following equation [44-46]:

$$K_\emptyset = \sum a_n cos^4 \theta_n \tag{35}$$

where a_n is the fraction of fibres with orientation angle, θ_n with respect to the loading direction [47]; K_{st} can be obtained from L_c from interfacial shear strength which can be obtained using a fibre fragmental and/or pull-out test . The Modified Cox and MROM show disparity with the

experimental strengths obtained for harakeke up to about 62% and 41% respectively. The difference between the predicted and the actual strengths for harakeke fibre composites obtained using the Modified Cox and Modified Rule of Mixtures can be seen to become larger as the fibre content increases up to 30wt% fibre, with better agreement at fibre content greater than 30 wt% than at 30 wt%. For hemp fibre composites, better agreement with experimental strengths compared to that harakeke fibre composite is observed; the highest differences were about 41 and 17% for the Modified Cox and MROM models respectively. The differences obtained here are not surprising given that similar large disparity with these models has also been reported in previous work with other natural fibre composites [48, 49], where generally lower values of K_θ have been used for less aligned fibre composites (as previously discussed K_θ is commonly taken as unity for axially aligned fibre composites, 0.375 for planar random configuration and 0.2 for a three dimensional randomly oriented fibre composites). General large disparity highlights potential fault with the assumptions for these models. Indeed, they are simplistic in nature and do not take account of failure mechanisms. A major oversight is that of the influence of stress concentrations on premature failure of composites as a result of different fibre orientations. It should be noted that the K_θ values used for the Modified Cox and MROM models are based on average fibre orientation, whereas some are oriented at very high angles to the loading direction. Furthermore, fibre debonding is also not taken account of, which could be expected to have a significant influence on strength. For the Modified Cox model, it is assumed that the interface between the fibre and the matrix is perfect [50]. High interfacial shear strength is generally indicated by matrix tearing/fibre fracture depending on failure strain of the material. According to Von Mises yield criterion, the shear stress (τ_m) required to bring about matrix tearing can be estimated from the tensile strength of the matrix using the following equation [24]:

$$\tau_m = \frac{\sigma_m}{\sqrt{3}} \tag{36}$$

where σ_m is the matrix tensile strength. Taking the tensile strength of PLA as 53.86 MPa, the obtained τ_m based on the Equation 36 is 31.1 MPa; this is higher than the interfacial strength obtained here (calculated using the Bowyer-Bader model) for harakeke and hemp fibre composites, suggesting that fibre debonding will occur during testing. The mechanism of pull-out is also neglected by these models. Furthermore, the fibre strength used in both models is the average fibre strength; in actual composites some fibres could fail at much lower stresses than the average fibre strength.

A comparison between the fitted, predicted and the experimental Young's moduli for harakeke and hemp fibre composites with different fibre contents are shown in Figure 10.

Figure 10

It can be seen that good fits (< 10%) between the theoretical and experimental values are obtained for the Hirsch model up to 25 wt% fibre with a noticeable increase in disparity at fibre contents higher than 25 wt%, which is believed to be due to fibre agglomeration. At fibre contents lower than 25 wt%, the differences are found to be relatively lower than those found in the literature for other discontinuous fibre composites for which there is a less linear trend for experimental values which can be explained by less uniform fibre distribution [42, 51]. The value of x (0.9) for harakeke and hemp fibre composites, however, is close to that which would be expected for continuous fibre composites (x=1) and higher than those for other discontinuous natural fibre composites made using injection moulding where lower values of x has commonly been used (0.2 – 0.8) [51-55], suggesting better reinforcement efficiency from fibre mats is

obtained. It is much higher than that obtained when fitting for strength (0.13); given that x is meant to represent stress transfer, this suggests that less stress transfer may be occurring at the point where strength is measured which occurs at higher stress (at which point debonding can be reducing stress transfer) than where Young's modulus is measured, which could explain to an extent the difference seen.

A good agreement between the predicted and the experimental Young's moduli is also obtained from the Modified Halpin-Tsai, with disparity of less than 10% up to fibre contents up to 25 wt% and higher at fibre contents higher than 25 wt% as seen for the Hirsch model. It is interesting to note that these predicted Young's moduli are obtained using the fitting parameter ζ according to the Equation 13 (111 for harakeke and 52 for hemp), which over-predicted strength (taken as 2 for strength), the higher value for ζ for Young's modulus compared to that for strength can again be attributed to the higher stress transfer at where Young's modulus is measured compared to where strength is measured. A good agreement with the experimental Young's modulus again suggests that reasonable fibre alignment is obtained when using a DSF, when considering that this model was developed for aligned fibre composites.

It can also be seen from Figure 7 that good agreement (within 6%) between Young's modulus predicted by the Cox model and experiment is obtained up to 25wt% fibre with increased disparity for fibre contents higher than 25 wt%, similar to that obtained for the Hirsch and Modified Halpin-Tsai models and much better accuracy than for prediction of strength by the Cox model. It is believed that at low stress at where Young's modulus is measured, much less or no fibre debonding occurs unlike for strength, so better agreement with the assumption used by the model that the interface between fibres and matrix is perfect. However, experimentally

the integrity of the fibre-matrix interfacial bonding reduced with the increment of the fibre content.

The Modified Cox and the MROM models are found to largely underestimate Young ‘s moduli (Figure 10). A similar discrepancy has also been observed in other work for discontinuous fibre composites for which discrepancies of up to 300% [56] and 60% [57] have been found for the Modified Cox and the MROM respectively. Differences predicted for Young’s modulus using the Modified Cox (71 and 120% for harakeke and hemp respectively) and the MROM (54 and 84% for harakeke and hemp respectively) models in this work are much larger than those obtained for strength. Large disparity obtained from these models is believed to be due to some extend values for stress transfer reduction factors, K_θ and K_{st} determined from composite strength (using the Bowyer-Bader model); the actual values for these stress transfer factors at low stress level where Young’s modulus is measured would be expected to be higher as discussed previously due to less (or no) debonding.

From the presented results for Young’s modulus, it is clearly observed that except for the Modified Cox and MROM, the predicted Young’s moduli obtained from the other models fit reasonably well with experiment, particularly for fibre contents less than 25 wt%, which is interesting considering these are simple models. It should be kept in mind that the assumptions made for Young’s modulus are much more accurate than for strength, and so simple prediction should be expected to be more accurate. However, it is acknowledged that larger discrepancy (up to 140%) has been seen in the literature when these models used to predict Young’s modulus for other natural fibre composites. The Cox model predicted Young’s modulus for harakeke

and hemp fibre composites best, as found generally in the literature which could be due to the fact that it takes more account of fibre (fibre radius) and matrix (shear modulus) properties.

5. CONCLUSION

Comparison between experimental results and the prediction from theory for the tensile properties of composites reinforced with these fibre mats have been presented. It was found that using a DSF to make fibre mats lead to better fibre alignment compared to that for composites made using injection moulding and composites reinforced with randomly oriented fibre mats. The Modified Cox and MROM models were found to give reasonable agreement with experimental tensile strength, while the Modified Halpin-Tsai and Cox models were found to be the best models that can be used to predict Young's modulus with disparity of less than 10% for composites with fibre content up to 25wt% taking into consideration the integrity of the fibre-matrix interfacial bonding.

ACKNOWLEDGEMENT

This research received no specific grant from any funding agency in the public, commercial, or not-for-profit sectors. However, the author would like to thank to the Composites Research Group, University of Waikato for their support and the Ministry of Higher Education and Universiti Teknologi Mara Malaysia for the scholarship.

REFERENCES

1. Dittenber, D.B. and H.V.S. GangaRao, *Critical Review of Recent Publications on Use of Natural Composites in Infrastructure*. Composites Part A: Applied Science and Manufacturing, 2011.
2. Ku, H., et al., *A review on the tensile properties of natural fiber reinforced polymer composites*. Composites Part B: Engineering, 2011. **42**(4): p. 856-873.
3. Kelly, A. and W. Tyson, *Tensile properties of fibre-reinforced metals: copper/tungsten and copper/molybdenum*. Journal of the Mechanics and Physics of Solids, 1965. **13**(6): p. 329-350.

4. Thomason, J., *Micromechanical parameters from macromechanical measurements on glass reinforced polyamide 6, 6*. Composites Science and Technology, 2001. **61**(14): p. 2007-2016.
5. Thomason, J., *The influence of fibre length and concentration on the properties of glass fibre reinforced polypropylene. 6. The properties of injection moulded long fibre PP at high fibre content*. Composites Part A: Applied Science and Manufacturing, 2005. **36**(7): p. 995-1003.
6. Li, Y., Y.-W. Mai, and L. Ye, *Sisal fibre and its composites: a review of recent developments*. Composites Science and Technology, 2000. **60**(11): p. 2037-2055.
7. Kalaprasad, G., et al., *Theoretical modelling of tensile properties of short sisal fibre-reinforced low-density polyethylene composites*. Journal of materials Science, 1997. **32**(16): p. 4261-4267.
8. Fuchs, C., et al., *Application of Halpin–Tsai equation to microfibril reinforced polypropylene/poly (ethylene terephthalate) composites*. Composite Interfaces, 2006. **13**(4-6): p. 331-344.
9. Halpin, J.C., *Effects of Environmental Factors on Composite Materials*. 1969, DTIC Document.
10. Facca, A.G., M.T. Kortschot, and N. Yan, *Predicting the elastic modulus of natural fibre reinforced thermoplastics*. Composites Part A: Applied Science and Manufacturing, 2006. **37**(10): p. 1660-1671.
11. Alhuthali, A. and I.M. Low, *Mechanical properties of cellulose fibre reinforced vinyl-ester composites in wet conditions*. Journal of materials Science, 2013. **48**(18): p. 6331-6340.
12. Tucker III, C.L. and E. Liang, *Stiffness predictions for unidirectional short-fiber composites: review and evaluation*. Composites Science and Technology, 1999. **59**(5): p. 655-671.
13. Landel, R.F. and L.E. Nielsen, *Mechanical properties of polymers and composites*. 1993: CRC Press.
14. Fu, S.-Y., B. Lauke, and Y.-W. Mai, *Science and engineering of short fibre reinforced polymer composites*. 2009: Elsevier.
15. Thomason, J., et al., *Influence of fibre length and concentration on the properties of glass fibre-reinforced polypropylene: Part 3. Strength and strain at failure*. Composites Part A: Applied Science and Manufacturing, 1996. **27**(11): p. 1075-1084.
16. Hull, D. and T. Clyne, *An introduction to composite materials*. 1996: Cambridge university press.
17. Piggott, M.R., *Load bearing fibre composites*. 2002: Springer Science & Business Media.
18. Cox, H., *The elasticity and strength of paper and other fibrous materials*. British journal of applied physics, 1952. **3**(3): p. 72.
19. Krenchel, H., *Fibre reinforcement - theoretical and practical investigation of the elasticity and strength of fibre-reinforced materials* 1964, Alademisk forlag: Copenhagen.
20. Sanadi, A. and M. Piggott, *Interfacial effects in carbon-epoxies*. Journal of materials Science, 1985. **20**(2): p. 421-430.
21. Thomason, J. and M. Vlug, *Influence of fibre length and concentration on the properties of glass fibre-reinforced polypropylene: 1. Tensile and flexural modulus*. Composites Part A: Applied Science and Manufacturing, 1996. **27**(6): p. 477-484.
22. Bader, M. and W. Bowyer, *An improved method of production for high strength fibre-reinforced thermoplastics*. Composites, 1973. **4**(4): p. 150-156.
23. Bowyer, W. and M. Bader, *On the re-inforcement of thermoplastics by imperfectly aligned discontinuous fibres*. Journal of materials Science, 1972. **7**(11): p. 1315-1321.
24. Beckermann, G. and K.L. Pickering, *Engineering and evaluation of hemp fibre reinforced polypropylene composites: fibre treatment and matrix modification*. Composites Part A: Applied Science and Manufacturing, 2008. **39**(6): p. 979-988.
25. Khalil, H., et al., *The effect of acetylation on interfacial shear strength between plant fibres and various matrices*. European Polymer Journal, 2001. **37**(5): p. 1037-1045.
26. Fu, S.-Y., et al., *Tensile properties of short-glass-fiber-and short-carbon-fiber-reinforced polypropylene composites*. Composites Part A: Applied Science and Manufacturing, 2000. **31**(10): p. 1117-1125.

27. Aziz, S.H. and M.P. Ansell, *The effect of alkalization and fibre alignment on the mechanical and thermal properties of kenaf and hemp bast fibre composites: Part 1–polyester resin matrix*. Composites Science and Technology, 2004. **64**(9): p. 1219-1230.
28. Aruan Efendy, M.G. and K. Pickering, *Comparison of Harakeke with Hemp Fibre as a Potential Reinforcement in Composites*. Composites Part A: Applied Science and Manufacturing, 2014.
29. Efendy, M.A. and K.L. Pickering, *Fibre orientation of novel dynamically sheet formed discontinuous natural fibre PLA composites*. Composites Part A: Applied Science and Manufacturing, 2016. **90**: p. 82-89.
30. Efendy, M.A. and K.L. Pickering, *Comparison of harakeke with hemp fibre as a potential reinforcement in composites*. Composites Part A: Applied Science and Manufacturing, 2014. **67**: p. 259-267.
31. Pickering, K. and M.A. Efendy, *Preparation and mechanical properties of novel bio-composite made of dynamically sheet formed discontinuous harakeke and hemp fibre mat reinforced PLA composites for structural applications*. Industrial Crops and Products, 2016. **84**: p. 139-150.
32. Krishnaprasad, R., et al., *Mechanical and thermal properties of bamboo microfibril reinforced polyhydroxybutyrate biocomposites*. Journal of Polymers and the Environment, 2009. **17**(2): p. 109-114.
33. Madsen, B. and H. Lilholt, *Physical and mechanical properties of unidirectional plant fibre composites—an evaluation of the influence of porosity*. Composites Science and Technology, 2003. **63**(9): p. 1265-1272.
34. Faruk, O., et al., *Biocomposites reinforced with natural fibers: 2000–2010*. Progress in polymer science, 2012. **37**(11): p. 1552-1596.
35. Graupner, N., *Improvement of the mechanical properties of biodegradable hemp fiber reinforced poly (lactic acid)(PLA) composites by the admixture of man-made cellulose fibers*. Journal of Composite Materials, 2009.
36. Efendy, M.A. and K. Pickering, *Comparison of harakeke with hemp fibre as a potential reinforcement in composites*. Composites Part A: Applied Science and Manufacturing, 2014. **67**: p. 259-267.
37. Joseph, P., K. Joseph, and S. Thomas, *Effect of processing variables on the mechanical properties of sisal-fiber-reinforced polypropylene composites*. Composites Science and Technology, 1999. **59**(11): p. 1625-1640.
38. Baghaei, B., et al., *Novel aligned hemp fibre reinforcement for structural biocomposites: Porosity, water absorption, mechanical performances and viscoelastic behaviour*. Composites Part A: Applied Science and Manufacturing, 2014. **61**: p. 1-12.
39. Krishnan, K.A., R. Anjana, and K. George, *Effect of alkali-resistant glass fiber on polypropylene/polystyrene blends: Modeling and characterization*. Polymer Composites, 2014.
40. Mathew, L. and R. Joseph, *Mechanical properties of short-isora-fiber-reinforced natural rubber composites: Effects of fiber length, orientation, and loading; alkali treatment; and bonding agent*. Journal of applied polymer science, 2007. **103**(3): p. 1640-1650.
41. Venkateshwaran, N. and A. ElayaPerumal, *Modeling and evaluation of tensile properties of randomly oriented banana/epoxy composite*. Journal of Reinforced Plastics and Composites, 2011: p. 0731684411430559.
42. Indira, K., J. Parameswaranpillai, and S. Thomas, *Mechanical properties and failure topography of banana fiber PF macrocomposites fabricated by RTM and CM techniques*. ISRN Polymer Science, 2013. **2013**.
43. Sreenivasan, V., et al., *Mechanical properties of randomly oriented short Sansevieria cylindrica fibre/polyester composites*. Materials & Design, 2011. **32**(4): p. 2444-2455.
44. Vallejos, M., et al., *Micromechanics of hemp strands in polypropylene composites*. Composites Science and Technology, 2012. **72**(10): p. 1209-1213.
45. Krenchel, H., *Fibre reinforcement*. 1964: Alademisk forlag.

46. Taha, I. and Y.F. Abdin, *Modeling of strength and stiffness of short randomly oriented glass fiber—polypropylene composites*. Journal of Composite Materials, 2011. **45**(17): p. 1805-1821.
47. Miao, M. and M. Shan, *Highly aligned flax/polypropylene nonwoven preforms for thermoplastic composites*. Composites Science and Technology, 2011. **71**(15): p. 1713-1718.
48. Garkhail, S., R. Heijenrath, and T. Peijs, *Mechanical properties of natural-fibre-mat-reinforced thermoplastics based on flax fibres and polypropylene*. Applied Composite Materials, 2000. **7**(5-6): p. 351-372.
49. Van den Oever, M., H. Bos, and M. Van Kemenade, *Influence of the physical structure of flax fibres on the mechanical properties of flax fibre reinforced polypropylene composites*. Applied Composite Materials, 2000. **7**(5-6): p. 387-402.
50. Piggott, M.R., *Short fibre polymer composites: a fracture-based theory of fibre reinforcement*. Journal of Composite Materials, 1994. **28**(7): p. 588-606.
51. Sreekumar, P., et al., *A comparative study on mechanical properties of sisal-leaf fibre-reinforced polyester composites prepared by resin transfer and compression moulding techniques*. Composites Science and Technology, 2007. **67**(3): p. 453-461.
52. Sawpan, M.A., *Mechanical Performance of Industrial Hemp Fibre Reinforced Polylactide and Unsaturated Polyester Composites*. 2010, The University of Waikato.
53. Vilaseca, F., et al., *Biocomposites from abaca strands and polypropylene. Part I: Evaluation of the tensile properties*. Bioresource technology, 2010. **101**(1): p. 387-395.
54. Beg, M.D.H., *The improvement of interfacial bonding, weathering and recycling of wood fibre reinforced polypropylene composites*. 2007, The University of Waikato.
55. López, J., et al., *PP composites based on mechanical pulp, deinked newspaper and jute strands: a comparative study*. Composites Part B: Engineering, 2012. **43**(8): p. 3453-3461.
56. Taha, I., A. El-Sabbagh, and G. Ziegmann, *Modelling of strength and stiffness behaviour of natural fibre reinforced polypropylene composites*. Polymers & Polymer Composites, 2008. **16**(5): p. 295.
57. Du, Y., et al., *Kenaf bast fiber bundle-reinforced unsaturated polyester composites. IV: effects of fiber loadings and aspect ratios on composite tensile properties*. Forest Products Journal, 2010. **60**(7): p. 582-591.

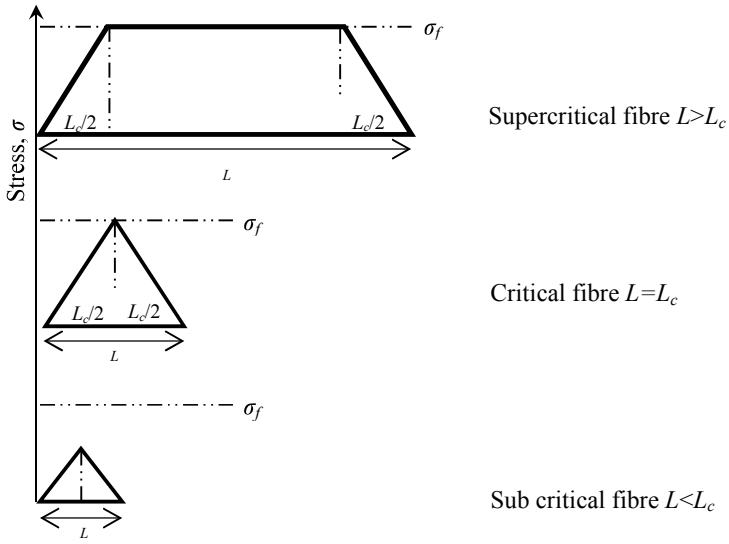

Figure 1: Schematic illustration indicating tensile stress distribution along the fibre having supercritical, critical and subcritical length embedded in elastic-perfectly plastic matrix.

Figure 2: Dynamic sheet former (DSF) used to produce aligned discontinuous fibre mats.

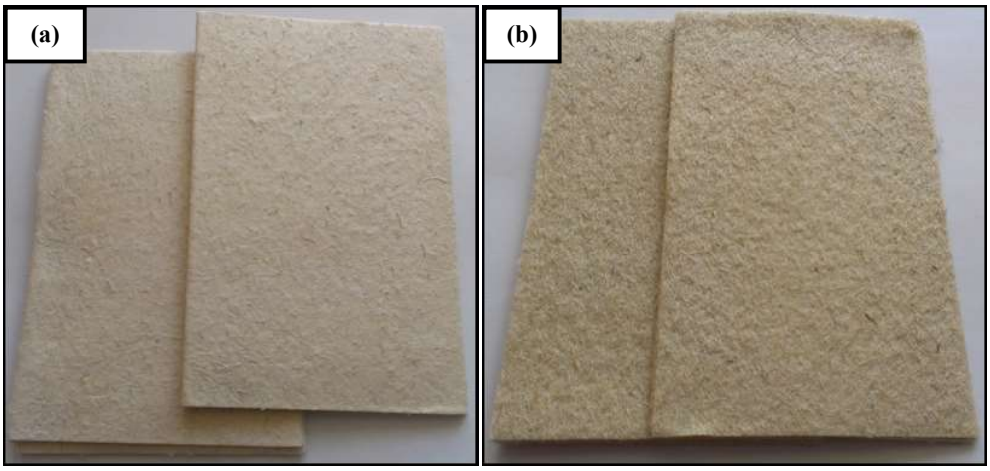

Figure 3: Fibre mats produced using DSF: (a) harakeke and (b) hemp.

Figure 4: Composites before (a) and after (b) cutting.

Figure 5: Typical fracture mode of samples.

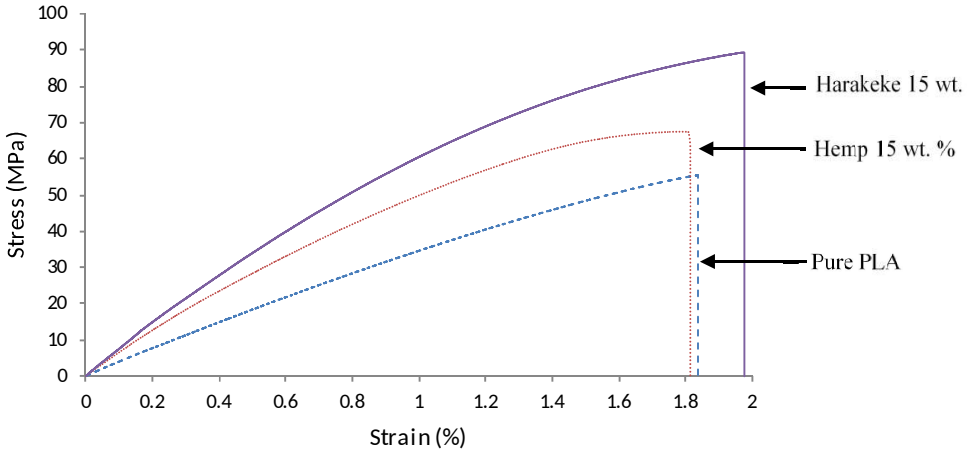

Figure 6: Typical stress versus strain curves for harakeke and hemp composites.

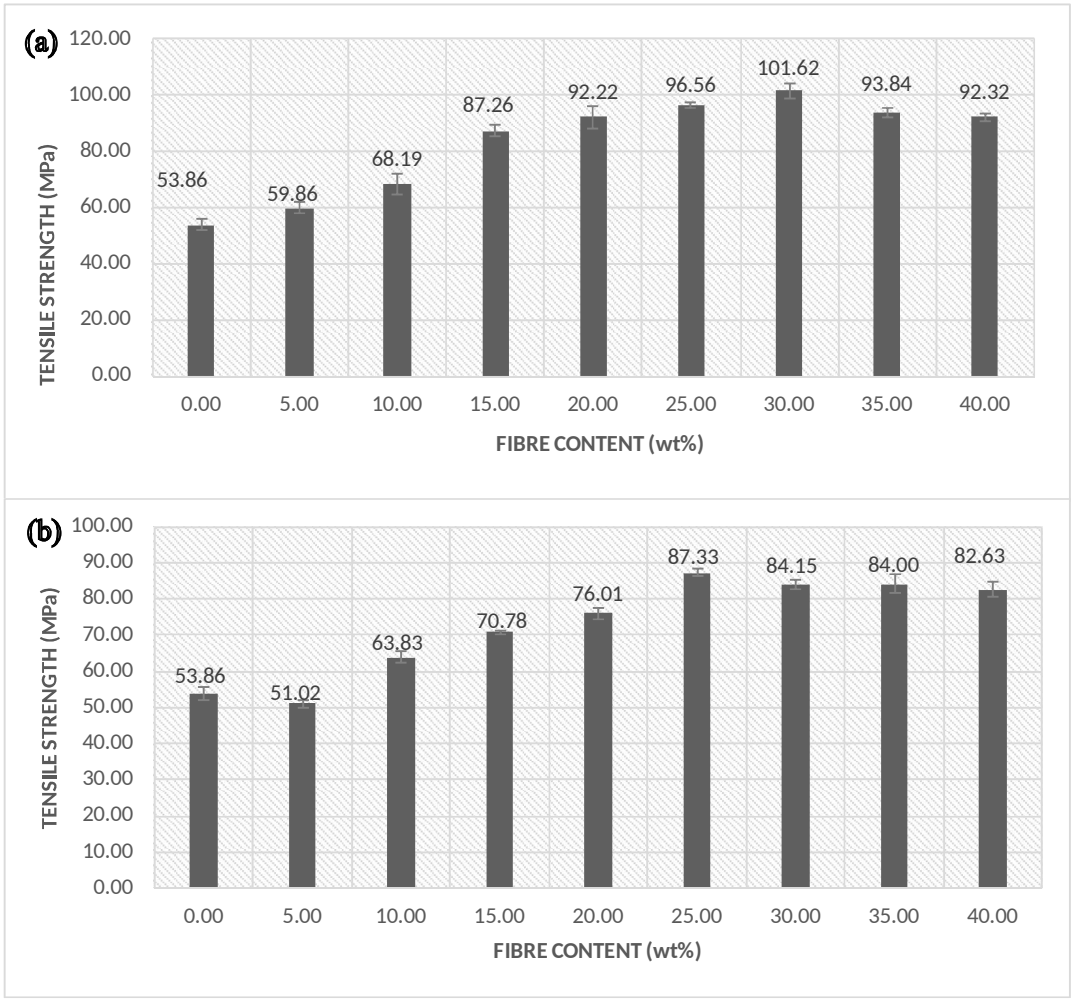

Figure 7: Tensile strength as a function of fibre content and loading direction for: (a) harakeke and (b) hemp reinforced PLA. Error bars each corresponds to one standard deviation.

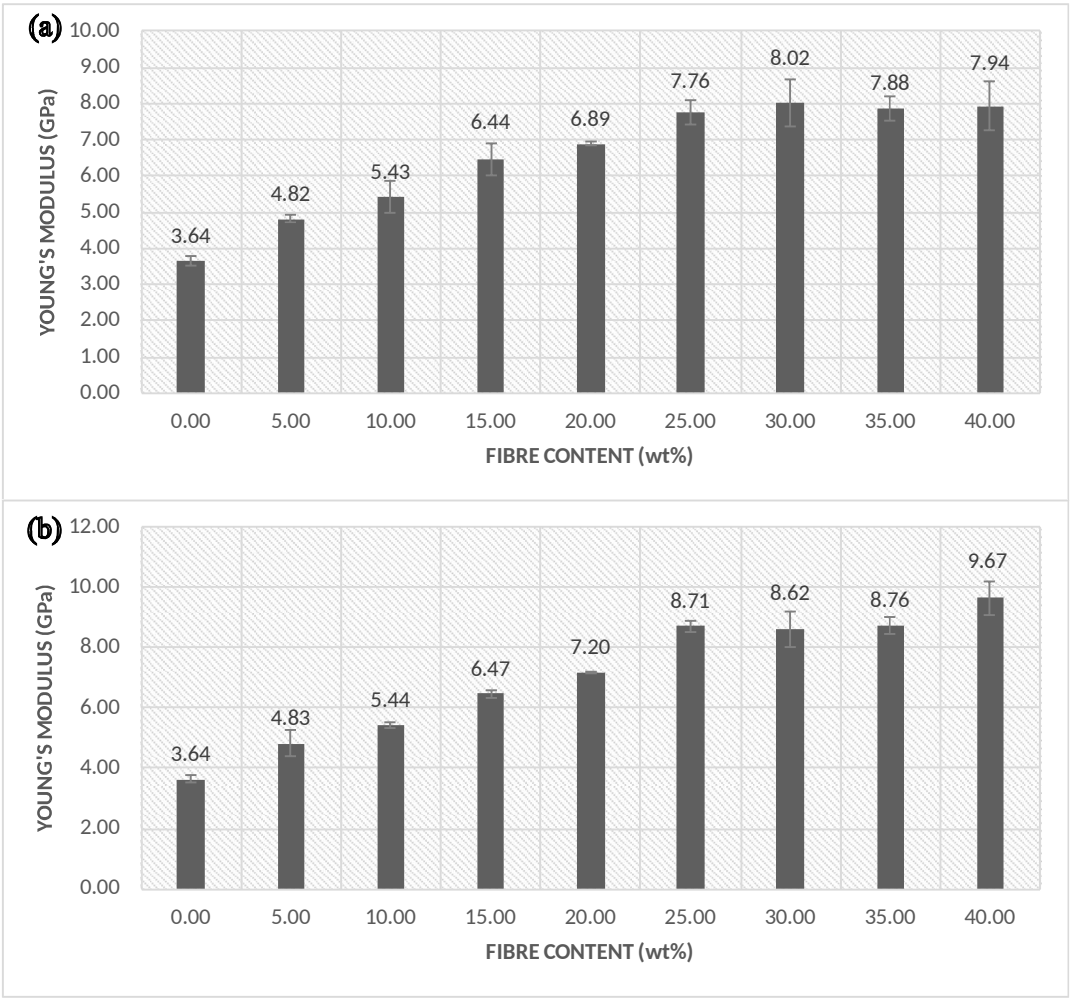

Figure 8: Young's moduli as a function of fibre content and loading direction for: (a) harakeke and (b) hemp reinforced PLA. Error bars each corresponds to one standard deviation.

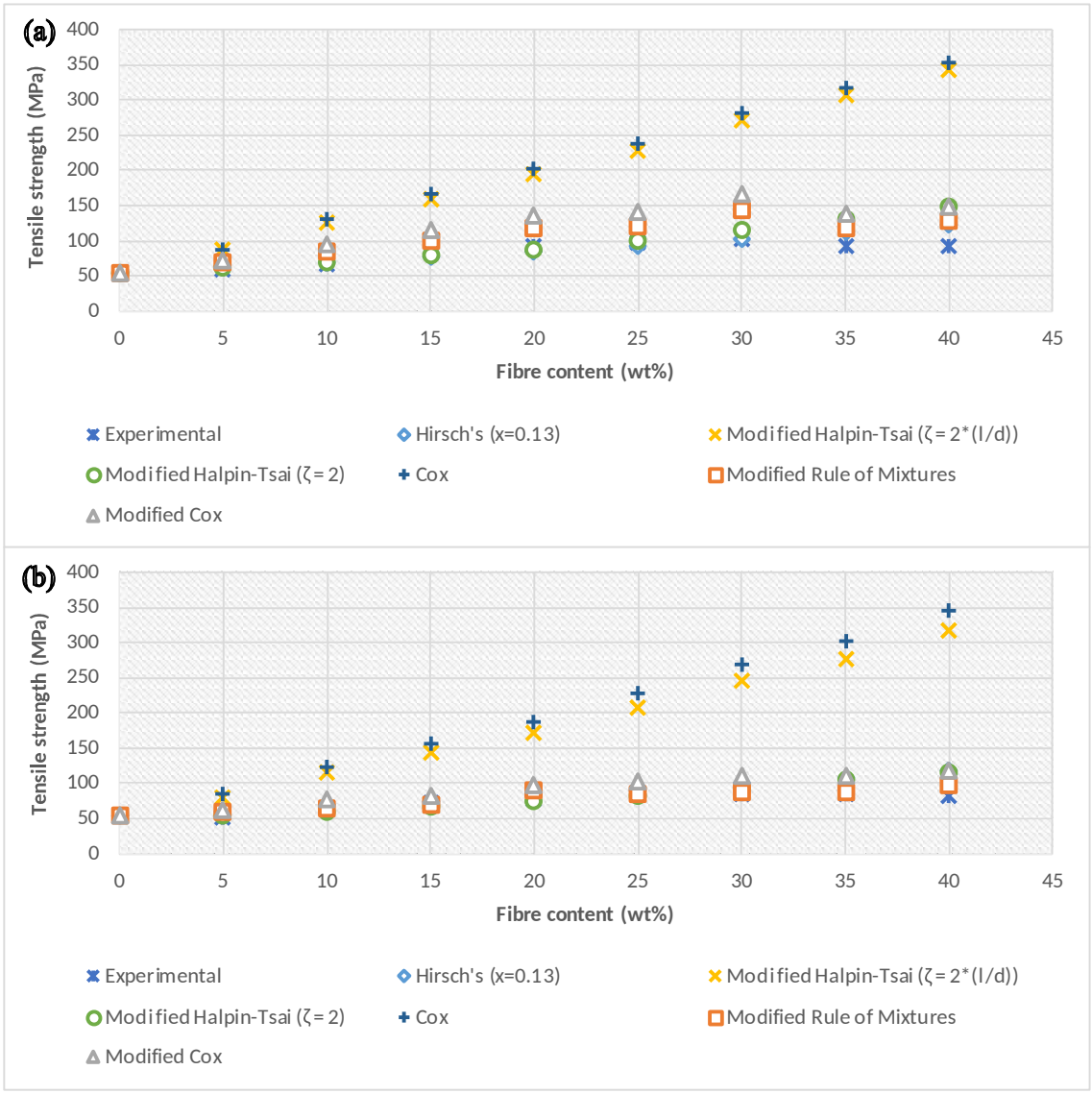

Figure 9: Variation of predicted and actual strengths composites taking into consideration fibre orientation factor for: (a) harakeke and (b) hemp fibre.

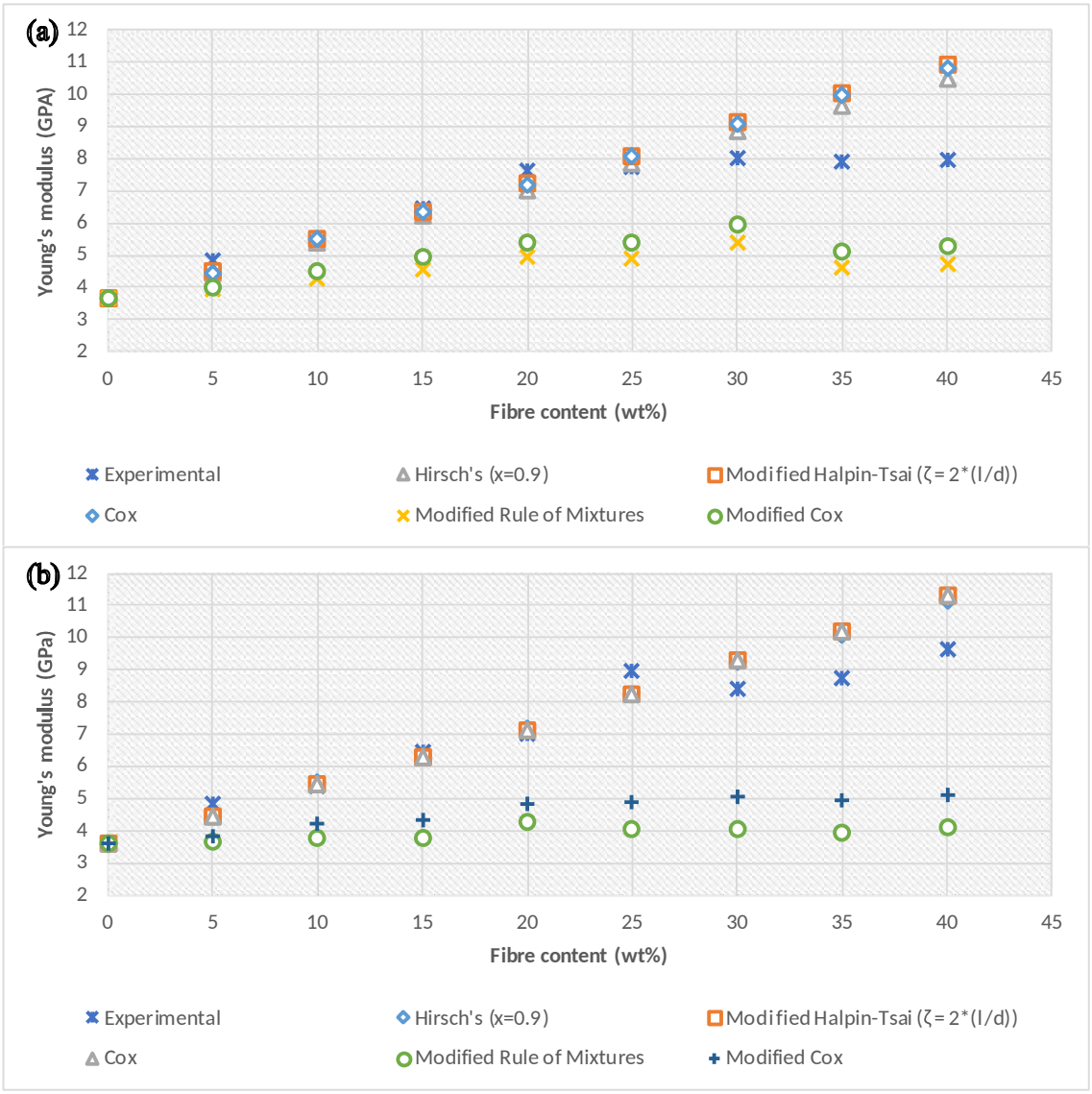

Figure 10: Variation of predicted and actual Young's moduli for: (a) harakeke and (b) hemp fibre.